Correlation between the morphology and photo-physical properties of P3HT:fullerene blends

David E. Motaung[1, 2], Gerald F. Malgas[1,*] and Christopher J. Arendse[2,†]

[1]National Centre for Nano-structured Materials, Council for Scientific Industrial Research, P. O. Box 395, Pretoria, 0001, South Africa

[2]Deparment of Physics, University of the Western Cape, Private Bag X17, Bellville, 7535, South Africa

ABSTRACT

The photo induced charge transfer and optoelectronic efficiency of the solar cells correlated to the morphology and the structure of P3HT:C_{60} blend was studied by means of photoluminescence (PL) and electron spin resonance (ESR). The occurrence of photoinduced charge transfer, well-known for blends of P3HT with fullerenes, was evidenced in blends of P3HT:C_{60} (1:1 wt. ratio) by a strong partially quenching of the P3HT luminescence. The ESR measurements allowed one to quantify the charge transfer between P3HT and C_{60}, which resulted in positive P3HT polarons. Wide angle x-ray scattering (WAXS) and UV-vis spectroscopy showed that an inclusion of a C_{60} fullerene in the P3HT matrix lead to lower peak intensities and dark Debye rings and a blue shift on the π–π^* interband transition of the P3HT as well as a reduction in the absorption coefficients. Selected area electron diffraction

* Corresponding Author: Dr. Gerald Malgas, Tel: (+27) 012 841 3972, Fax: (+27) 012 841 2229, Email: gmalgas@csir.co.za
† Corresponding Author: Prof. Christopher Arendse, Tel: (+27) 021 9593473, Fax: (+27) 021 959 2327, Email: cjarendse@uwc.ac.za

patterns of a well-ordered sample of P3HT exhibit distinct diffraction rings indicating that the P3HT forms a polycrystalline film. The large-scale phase separation of P3HT and C_{60} resulted from large C_{60} agglomerations during spin coating lead to a low power conversion efficiency of 0.2×10^{-4} %.

Keywords: Poly(-3-hexylthiophene); optical properties; regioregularity; morphology; solar cells.

1. INTRODUCTION

Since the discovery of charge separation in polymer/fullerene systems by Sariciftci *et al*. **[1]**, organic photovoltaics (OPVs) became one of the most promising alternative concepts of the solar cells-based crystalline silicon technology. This is due to their low cost, low temperature processing, flexibility and a very high speed of processing **[2]**. The technology of polymer photovoltaics has seen some drastic improvements in their power conversion efficiency with the introduction of the bulk heterojunction consisting of an interpenetrating network of electron donor (D) and acceptor (A) materials **[3, 4]**. Power conversion efficiencies in the range of 6.5 % have been achieved **[5]** successfully through selection of materials with suitable energy levels, control of nano-morphology **[6]** either during film deposition **[7]** or using post-fabrication procedures such as thermal annealing **[8, 9-14]** and by optimisation of electrode materials **[15]**.

Such progress makes polymer solar cells more competitive with amorphous silicon based solar cells. The main factors that limit the performance of polymer solar cells are charge carrier transport **[16],** narrow absorption in the visible range of the solar spectrum of the active layer and low open circuit voltages **[17, 18]**. In general, bicontinuous nanoscale morphology is pleasing for the D/A acceptor junctions, and high crystallinity in the D/A phases is also essential for better transportation ability of the charge carrier. Though, the ideal bicontinuous two-phase nanoscale morphology is difficult to obtain due to reduced solubility of the fullerene and inappropriate phase separation during the film cast process. Currently, several works have been reported on making nanorods or nanowires structures of P3HT or C_{60} to form a three-dimensional (3D) interpenetrating network such as the formation of fullerene nanorods structure with different sizes by solvent-vapour treatments at different vapour pressures **[19]**.

These approaches provide promising protocols for morphology manoeuvring of conjugated polymer/C_{60} for solar cells to obtain better charge carrier mobility and increase the absorption of solar energy. The C_{60} derivative; PCBM was mainly used in published works, due to its higher solubility. However, C_{60} may be a good candidate for an efficient acceptor material due to its higher electron mobility and crystalline structure compared to PCBM. The morphology fabrication of P3HT/C_{60} blends remains a fundamental challenge in the field of conjugated polymer/C_{60} solar cells **[19, 20]**. In this article, photo induced charge transfer and optoelectronic

properties of photovoltaic cells correlated to the morphology and the structure of P3HT:C_{60} blend was studied in detail.

2. EXPERIMENT DETAILS

2.1. *Materials*

A regioregular poly (3-hexylthiophene) (rr-P3HT) polymer with a molecular weight (M_w) of ~64,000 $gmol^{-1}$; with regularity that is greater than 98.5 % for head-to-tail, buckminsterfullerene-C_{60} with a purity of 99.5%, Indium tin oxide (ITO) coated on a 1 mm glass substrate with a sheet resistance of 8-12 Ω/sq^{-1}, poly (3,4-ethylenedioxythiophene):poly (styrenesulfonate) (PEDOT:PSS), and a chloroform ($CHCl_3$) solution were purchased from Sigma-Aldrich.

2.2. Sample preparation

All materials used in this study were used as received, without any further purification. Regioregular P3HT was used as an electron donor material; while a fullerene-C_{60} was used as an electron acceptor material. A mixture of rr-P3HT (5 mg) and C_{60} (5 mg) dissolved in 1mL of $CHCl_3$ solution was stirred over night at a temperature of 50 °C in order to promote a complete dissolution. It should be noted that the solubility of C_{60} fullerene on chloroform is about 0.16 mg/mL **[21]**.

For solar cells fabrication, a thin layer of PEDOT:PSS solution was spin coated onto the ultrasonically cleaned ITO glass substrates and silicon (Si)

substrates with the spin rate of 2500 rpm for 30 s. This was followed by thermal treatment of the substrates at 100 °C for 30 min. The P3HT and blend films with a thickness of about 100 nm was spin coated onto the PEDOT:PSS layer. The spinning rate and time of spin-coating were 2500 rpm and 30 sec, respectively. The samples were dried on a hot plate at a temperature of 50 °C for 15 min to dry (or evaporate) the excess solvent. Solar cells were completed by evaporating about 100 nm of aluminium (Al) on top of the active layer (ITO/P3HT:C_{60} (1:1 wt. ratio)/Al) through a shadow mask by means of thermal evaporation in vacuum at a pressure of about 5×10^{-4} Pa resulting in an active device area of 0.14 cm^2.

2.3 Characterization

Surface morphological studies of P3HT and P3HT:C_{60} (1:1 wt ratio) were carried out using an atomic force microscope (AFM) and a LEO 1525 SEM, operated at an accelerating voltage of 5 kV. The AFM images of the polymer films were acquired using a Veeco NanoScope IV Multi-Mode AFM with the tapping mode. A JEM-2100 JEOL high resolution transmission electron microscope (HR-TEM), operated at 100 kV was employed to examine the internal structure of the P3HT and the blends. Specimens for HR-TEM analysis were prepared by a placing a drop of P3HT dispersed in $CHCl_3$, onto a holey-carbon copper (Cu) grid and dried at ambient conditions. In order to determine the structural modification during heating; wide angle x-ray scattering (WAXS) measurements were performed using an Anton Paar SAXSess instrument, operating at an accelerating voltage of 40 kV and current of 50 mA. A Nickel (Ni) filtered CuK_α radiation source (0.154nm)

(PW3830 x-ray generator PANanalytical) radiation was used. Intensity profiles were obtained with a slit collimated compact Krathy Camera and recorded with a two-dimensional (2-D) imaging plate. Sample to detector distance was 264.5 mm and covers the length of the scattering angle (2θ) from 0.1 to 30 º. The samples were heated in a paste cell at room temperature and 110 ºC by a TCU50 (Anton-Paar) temperature control unit, which is attached to the SAXSess instrument.

The optical absorption study of spin-coated films was investigated by means of PekinElmer Lamda 750S Ultraviolet-visible (UV-vis) spectrophotometer. The photoluminescence measurements were carried out at room temperature by exciting the samples with the 350 nm deuterium lamp. The emission was detected with Jobin-Yvon PMT detector. It should be noted that for some PL measurements, the PEDOT:PSS layer was omitted in order to avoid masking of P3HT features which overlap with those of PEDOT. The film thickness was determined by α-stepper DEKTAK 6M Stylus profilometer (Veeco instruments). Electron spins resonance (ESR) measurements were performed with a JEOL, X-band spectrometer JES FA 200 equipped with an Oxford ESR900 gas-flow cryostat and a temperature control (Scientific instruments 9700). Measurements were done at room temperature (23 ºC). The power of 6.0 mW and frequency of 9.46 GHz were used.

The current density–voltage (*J*–*V*) characteristics of the polymer based organic solar cells were measured both in the dark and under illumination using a Keithley 2420. The devices were irradiated at 100 mW cm^{-2} using a

xenon lamp-based Sciencetech SF150 150W solar simulator equipped with an AM1.5 filter as the white light source; the optical power at the sample was 100 mW cm^{-2}, detected using a daystar meter. All the photovoltaic properties were evaluated in ambient air conditions at room temperature. The solar cells were illuminated through the side of the ITO-coated glass plate.

3. RESULTS AND DISCUSSION

The morphology of polymer/fullerene photo-active layers that plays a key role in the final solar cell performance was investigated using scanning electron microscopy (SEM) analysis. Figure 1 shows the SEM micrographs of the surface of P3HT and blended films spin-coated from a $CHCl_3$ solvent onto a silicon substrate. It is evident in Figure 1(a) that the P3HT film shows a less ordered morphology with pores uniformly across the film surface. Smooth surface for the P3HT film prepared from pyridine-chloroform solution was observed by Verma *et al*. **[22]**. The micrograph in Figure 1(b) shows that the surface has clusters/agglomerates of C_{60} fullerene in the polymer matrix which is uniformly distributed across the surface.

It is suggested that these clusters are nucleation sites for charge carrier transport and reduces the distance travelled by excitons to the respective polymer/C_{60} interface which greatly enhancing the effectiveness of photo-induced charge transfer from the polymer to C_{60}. Large agglomerated nanotubes in a P3HT film blended with a non functionalized single walled

carbon nanotubes (non-FSWCNTs–P3HT) were observed by Kumar *et al*. **[23]**.

To complement the HR-SEM analysis, AFM measurements were performed on the samples. Figure 2 presents 2-D and 3-D height images of P3HT and blended film of P3HT:C_{60} in a 1:1 wt. ratio. It is clear in Figure 2(a) that the sample show pores with diameters ranging from 70-100 nm and lengths/depth that ranges between 3.5 and 9.0 nm. A series of small clusters is observed in the P3HT:C_{60} blended film (Fig. 2(b)), which may be attributed to the C_{60} aggregates. The surface of P3HT and P3HT:C_{60} (1:1 wt. ratio) films shows a root mean square (rms) roughness of 2.194 and 4.202 nm, respectively. It has been reported that the D/A blend morphology can be controlled by spin-casting the blend from a specific solvent preventing large-size phase separation or enhancing the polymer chain packing **[6, 24]**.

High resolution TEM was used to further study the details of ordering of the P3HT active layer as shown in Figure 3. The inset in Fig. 3(a) corresponds to the (200) reflection, with a d-spacing of 0.86 nm. The selected area electron diffraction (SAED) pattern (Fig. 3(b)) of a well-aligned sample of P3HT exhibits distinct diffraction rings (spots) indicating that the P3HT forms a polycrystalline film. The P3HT structure shows the (100), (300) as well as the (010) reflections, with a d-spacing of 1.73, 0.52 and 0.37 nm, plane respectively, which are consistent with the WAXS results.

The microstructure and domain spacing for P3HT and blend were examined using wide-angle x-ray scattering technique (WAXS). Representative WAXS patterns for the as prepared P3HT and its blended samples measured at room temperature (RT) and heated at 110 ºC are presented in Figure 4 and 5. It is noticeable in Figure 4 and 5 that P3HT depicts its characteristic peaks at 2θ ≈ 5.2, 10.7, 16.3 and 23.4 º at RT, with broadly bright Debye rings of (*h00*) assigned to (100), (200) (300) and (010) reflections **[25]**.

The P3HT:C_{60} (1:1 wt. ratio) blend in Figure 4 and 5 (c, d) shows low peak intensities and diffused Debye rings of (100) and (010) crystalline reflections assigned to P3HT and (111), (220), (311) assigned to C_{60} fullerene. This indicates that the blended sample has low crystallinity and less ordered structure crystal orientation than a pure P3HT sample. The intensity of the (100) reflection due to lamella layer structure (1.64 nm) is strong, while the intensity of the (010) reflection due to π-π interchain stacking (0.38 nm) is very weak **[26]**.

The C_{60} diffraction patterns (Fig 5 (e, f)) are consistent with results obtained for buckminsterfullerene **[25, 27-29]**, which is known to have a face-centred-cubic (fcc) crystal structure at room temperature, and shows reflections for the (111), (220), (311), (222) and (331) diffraction peaks at 10.6, 17.7, 20.9, 21.7 and 27.4° **[25, 27-29]**. From the WAXS patterns of P3HT and the blended sample, the d-spacing ranges between 0.37 and 1.96

nm, and were estimated using Bragg's law **[30]**, while the crystal sizes were estimated using Scherrer's relation **[31]** as shown in Table 1.

However, when the P3HT sample is heated at a temperature of 110 ºC, diffraction peaks shift to lower angles (2θ ≈ 4.7, 9.8 and 16.0 º), giving a, significant increase in *d*-spacing and grain sizes of the (100) plane, as depicted in Table 1. This indicates an increase in the ordering of the alkyl chains within the main thiophene chains. It is interesting to note that at 110 ºC a broad peak formed around 17.1 º with a d-spacing and crystal size of 0.51 nm and 1.99 nm, respectively (Figure 4). The formation of this peak is clear in Figure 5(b) as indicated by an arrow.

Figure 6 compares the optical absorption coefficients spectra of rr-P3HT films with C_{60} fullerene and a blend of P3HT:C_{60} in a (1:1 wt. ratio) spin coated on an ITO glass substrate. Both polymers showed the band gap edge at 1.9 eV which is in agreement to the literature **[32-35]** and an absorption maximum at around 2.4 eV, which is characteristic of the π–π^* transition between the highest occupied π electron band and the lowest unoccupied one of the polymer **[36]**.

The development of a vibronic structure is also observed (refer to the shoulders peak around 2.25 eV and 2.06 eV), which is generally explained by a higher crystallization or ordering of intra-chain interactions in semiconducting polymers **[37, 38]**. The C_{60} fullerene shows a small absorption peak at around 3.31 eV. Upon blending the polymer with a C_{60} fullerene, a distinctive change in the peak wavelength is observed.

A blue shift on the π–π* interband transition of the P3HT blend as well as a reduction in the absorption coefficients is observed **[35]**. This is probably due to an altering in the stacking conformation of the polymer structure and a reduction of intraplane and interplane stacking, which causes a reduced π–π* transition and a lower absorbance (Fig. 6). Chirvase *et al*. **[39]** reported that the modification in the absorption spectra of P3HT:PCBM composite films is due to the presence of PCBM which destructs the ordering in the P3HT chains.

Photoluminescence (PL) measurements were carried out extensively to evaluate the effectiveness of the photo-induced charge transfer in an electron donor-acceptor pair. The PL spectra of P3HT and its blend with C_{60} fullerene measured at room temperature (RT) are shown in Figure 7. The P3HT film shows a strong PL signal around 1.75 eV and a shoulder around 1.92 eV which are assigned to the first vibronic band and the pure electronic transition respectively **[40-43]**. The PL emission peak in the shorter energy region (~1.55 eV) indicates an ordering in the P3HT lamella structure within the spherulites **[40-43]**. It is evident in Figure 8 that, when fullerene is added in the P3HT matrix, the intense photoluminescence of the P3HT is almost completely quenched. The luminescence studies indicate a profound photoinduced charge transfer in the bulk of P3HT:C_{60} (1:1 wt. ratio) blended film.

The effective charge separation in the P3HT:C_{60} (1:1 wt. ratio) system has been studied by ESR (electron spin resonance) signals. The spectrum of the blended film shown in Figure 8 was extracted at a microwave power of 6.0 mW in the dark at room temperature. Large ESR signal caused by a partial charge transfer is observed between rr-P3HT and fullerene in the dark state **[44, 45]**. Only rr-P3HT signals can be observed at room temperature, due to the spin-relaxation time for the C_{60} anions is short. The g-factor of the P3HT sample is about 2.0020, which can be attributed to the positive polarons in P3HT (P^+). These results are in good agreement with that obtained in the literature **[46, 47]**. A peak to- peak line width (ΔH_{pp}= 9 G) is observed for the blend. This indicates that rr-P3HT orientation is disturbed **[48]**, caused by the incomplete mixing of C_{60} as shown in the SEM (Fig. 1b). More detailed discussion, however, is beyond the scope of this work.

Figure 9 presents the current density-voltage (J-V) characteristics of a P3HT:C_{60} (1:1 wt ratio) device measured in the dark and under AM1.5 conditions with a white light illumination. The device achieved a short-circuit current density (J_{sc}) of 2.55 μAcm^{-2}, an open circuit voltage (V_{oc}) of 0.092 V, the fill factor of 0.20 and a final power conversion efficiency of about 0.2×10^{-4} %. The low V_{oc}, J_{sc} and efficiency may be attributed to the formation of large-size C_{60} crystals (Fig. 1), which causes not only a large-scale phase separation between P3HT and C_{60}, but also a rough P3HT:C_{60} (1:1 wt ratio) blend film as depicted in Figure 2. The rough P3HT:C_{60} layer may form some shunt paths after the top electrode deposition resulting in a low open circuit voltage.

Moulé *et al*. **[49]** reported that the morphology of the active layer strongly influences the performance of bulk heterojunction (BHJ) polymer solar cells. Previous studies of polycrystalline perylene diimide films have demonstrated exciton diffusion lengths of up to 2.5 μm **[50]**. However, the exciton diffusion length in conjugated polymers is merely about 10 nm, which are several orders of magnitude smaller than that in perylene diimide polycrystals. Therefore, the large phase separation of P3HT:C_{60} blend device might causes inefficient charge separation of excitons created in P3HT due to its short diffusion lengths.

4. CONCLUSION

In conclusion, we investigated the photo induced charge transfer correlated to the morphology and the structure of P3HT:C_{60} blended organic solar cells. The occurrence of photo-induced charge transfer was evidenced in blends of P3HT:C_{60} (1:1 wt. ratio) by a strong partially quenching of the P3HT luminescence. The ESR measurements allowed one to quantify the charge transfer between P3HT and C_{60}, which resulted in positive P3HT polarons. Wide angle x-ray scattering (WAXS) data and UV-vis spectroscopy showed that an incorporation of C_{60} in P3HT matrix lead to lower peak intensities, dark Debye rings and a blue shift on the π–π* interband transition of the P3HT as well as a reduction in absorption coefficients. The shift in diffraction peaks to lower angles, giving a significant increase in *d*-spacing and grain sizes of the (100) plane for films evaluated at 110 ° C was observed. The large-scale phase separation of P3HT and C_{60} resulted from

large C_{60} agglomerations during spin coating were observed by AFM and SEM leading to low power conversion efficiency of 0.2×10^{-4} %.

5. AKNOWLWDGEMENTS

The authors would like to thank the financial support of the Department of Science and Technology (DST) of South Africa and the Council for Scientific Industrial Research (CSIR), South Africa (Project No. HGERA7S). The authors are also grateful to Mrs. Jayita Bandyopadhyay and Mr. Thomas Malwela for their help and assistance with the small angle x-ray scattering and atomic force microscopy analysis.

6. REFERENCES

[1] N. S. Sariciftci, L. Smilowitz, A. J. Heeger, F. Wudl, Science 258 **(1992)** 1474.

[2] E. Bundgaard, F. C. Krebs, Sol. Energy Mater. Sol. Cells 91 **(2007)** 954–985.

[3] G. Yu, J. Gao, J. C. Hummelen, F. Wudl, A. J. Heeger, Science 270 **(1995)** 1789.

[4] Special Issue: Organic-Based Photovoltaics, MRS Bull. 30 (2005) issue 1**,**

[5] J. Y. Kim, K. Lee, N. E. Coates, D. Moses, Thuc-Quyen Nguyen, M. Dante, A. J. Heeger Science 317 **(2007)** 222.

[6] S. E. Shaheen, C. J. Brabec, N.S. Sariciftci, F. Padinger, T. Fromherz, J. C. Hummelen, Appl. Phys. Lett. 78 **(2001)** 841

[7] G. Li, V. Shortriya, J. Huang, Y. Yao, T. Moriarty, K. Emery, Y. Yang, Nat. Mater. 4 **(2005)** 864.

[8] W. L. Ma, C. Y. Yang, X. Gong, K. H. Lee, A. J. Heeger, Adv. Funct. Mater. 15 **(2005)** 1617

[9] F. Padinger, R. S. Ritterberger, N. S. Sariciftci, Adv. Funct. Mater. 13 **(2003)** 85.

[10] Y. Kim, S. A. Choulis, J. Nelson, D. D. C. Bradley, S. Cook, J.R. Durrant, Appl. Phys. Lett. 86 **(2005)** 063502.

[11] Y. Kim, S. Cook, S. M. Tuladhar, J. Nelson, J.R. Durrant, D. D. C. Bradley, M. Giles, I. McCulloch, M. Ree, C. S. Ha, Nat. Mater. 5 **(2006)** 197.

[12] C. J. Ko, Y. K. Lin, F. C. Chen, Adv. Mater. 19 **(2007)** 3520

[13] M. Reyes-Reyes, K. Kim, J. Dewald, R. López-Sandoval, A. Avadhanula, S. Curran, D.L. Carroll, Org. Lett. 7 **(2005)** 5749.

[14] P. Peumans, S. Uchida, S. R. Forrest, Nature 425 **(2003)** 158.

[15] M. D. Irwin, D. B. Buchholz, A. W. Hains, R. P. H. Chang, T. J. Marks, Proc. Nat. Acad. Sci. 105 **(2008)** 2783.

[16] W. L. Wang, H. B. Wu, C. Y. Yang, C. Luo, Y. Zhang, J. W. Chen, Y. Cao, Appl. Phys. Lett. 90 **(2007)** 183512.

[17] M. A. Loi, S. Toffanin, M. Muccini, M, Forster, U. Scherf, M. Scharber, Adv. Funct. Mater. 17 **(2007)** 2111.

[18] C. P. Chen, S. H. Chan, T. C. Chao, C. Ting, B. T. Ko, J. Am. Chem. Soc. 130 **(2008)** 12828.

[19] G. Lu, L. Li, X. Yang, Small 4 **(2008)** 601.

[20] X. N. Yang, G. H. Lu, L. G. Li, E. L. Zhou, Small 3 **(2007)** 611.

[21] R. S. Ruoff, D. S. Tse, R. Malhotra, D. C. Lorents, J Phys Chem. 97 **(1993)** 3379.

[22] D. Verma, V. Dutta, J. Renewable Sustainable Energy 1 **(2009)** 023107.

[23] J. Kumar, R. K. Singh, V. Kumar, R.C. Rastogi , R. Singh, Diamond & Related Materials 16 **(2007)** 446–453

[24] J. K. J. van Duren, X. Yang, J. Loos, C. W. T. Bulle-Lieuwma, A.B. Sieval, J. C. Hummelen, R. A. J. Janssen, Adv. Funct. Mater. 14 **(2004)** 425.

[25] International Centre for Diffraction Data (ICDD): P3HT (48-2040), C_{60} fullerene (47-0787, 44-0558).

[26] T. J. Prosa, M. J. Winokur, J. Moulton, P. Smith, A. J. Heeger, Macromolecules 25 **(1992)** 4364–4372.

[27] P. A. Heiny, J. E. Fischer, A. R. McGhie, W. J. Romanow, A. M. Denenstein, J. P. Jr. McCauley, A. B.III. Smith, D. E. Cox, Phys. Rev. Lett. 66 **(1991)** 2911–2914.

[28] M. E. Cagiao, A. O. Pozdnyakov, M. Krumova, V. V. Kudryavtsev, F. Balta Callej, J. Compos. Sci. Technol. 67 **(2007)** 2175–2182.

[29] J. Q. Li, Z. X. Zhao, Y. L. Li, D. B. Zhu, Z. Z. Gan, D. L. Yin, Physica C, 196 **(1992)** 135–140.

[30] B. E Warren, X-Ray Diffraction (New York: Dover) **(1990)** 251.

[31] B. D. Cullity, Elements of X-Ray Diffraction, 2nd ed.; Addison-Wesley Publishing Co.: Reading, MA, **(1978)**.

[32] T. Ahn, B. Choi, S. H. Ahn, S. H. Han, H. Lee, Synth. Met. 117 **(2001)** 219.

[33] G. Dicker, T. J. Savenije, B.-H. Huisman, D. M. de Leeuw, M. P. de Haas, J. M. Warman, Synth. Met. 137 **(2003)** 863.

[34] J. J. Apperloo, R. A. J. Janssen, M. M. Nielsen, K. Bechgaard, Adv. Mater. 12 **(2000)** 1594.

[35] W. R. Salaneck, I. Lundstrom, B. Ranby (Eds.), Conjugated Polymers and Related Materials Proceedings of the Eighty-first Nobel Symposium, Oxford University Press, **(1993)**, p. 290.

[36] X. Jiang, R. Osterbacka, O. Korovyanko, C. P. An, B. Horowitz, R. A. J. Janssen, Z. V. Vardeny, Adv. Funct. Mater. 12 **(2002)** 587.

[37] P. J. Brown, D. S. Thomas, A. Kohler, J. S. Wilson, J. S. Kim, C. M. Ramsdale, H. Sirringhaus, R. H. Friend, Phys. Rev. B 67, **(2003)** 064203.

[38] T. C. Chung, J. H. Kaufman, A. J. Heeger, F. Wudl, Phys. Rev. B 30 **(1984)** 702.

[39] D. Chirvase, J. Parisi, J. C. Hummelen, Nanotechnology 15 **(2004)** 1317.

[40] M. Sharma, D. Kaushik, R.R. Singh, R.K. Pandey, J. Mater. Sci.: Mater. Electron. 17 **(2006)** 537.

[41] D. E. Motaung, G. F. Malgas, C. J. Arendse, S. E. Mavundla, D. Knoesen, Materials Chemistry and Physics 116 **(2009)** 279–283

[42] L. Li, C.-M. Chan, K. L. Yeung, J.-X. Li, K.-M. Ng, Y. Lei, Macromolecules 34 **(2001)** 316.

[43] H. Yang, T. Shin, J.L. Yang, K. Cho, C.Y. Ryu, Z. Bao, Adv. Funct. Mater. 15 **(2005)** 671.

[44] K. Marumoto, N. Takeuchi, S. Kuroda, Chem. Phys. Lett. 382 **(2003)** 541.

[45] K. Marumoto, N. Takeuchi, T. Ozaki, S. Kuroda, Synth. Met. 129 **(2002)** 239.

[46] R. Dietmueller, A. R. Stegner, R. Lechner, S. Niesar, R. N. Pereira, M. S. Brandt, A. Ebbers, M. Trocha, H. Wiggers, M. Stutzmann, App. Phys. Lett. 94, **(2009)** 113301- 113303

[47] K. Marumoto, Y. Muramatsu, Y. Nagano, T. Iwata, S. Ukai, H. Ito, S. Kuroda, Y. Shimoi, S. Abe, J. Phys. Soc. Jpn. 74 **(2005)** 3066

[48] S. Watanabea, H. Tanaka, H. Ito, K. Marumoto, S. Kuroda, Synthetic Metals 159 **(2009)** 893–896

[49] A. J. Moulé, K. Meerholz, Adv. Mater. 20 **(2008)** 240.

[50] J. J. Dittmer, E. A. Marseglia, R. H. Friend, Adv. Mater. 12 **(2000)** 1270.

Figure 1

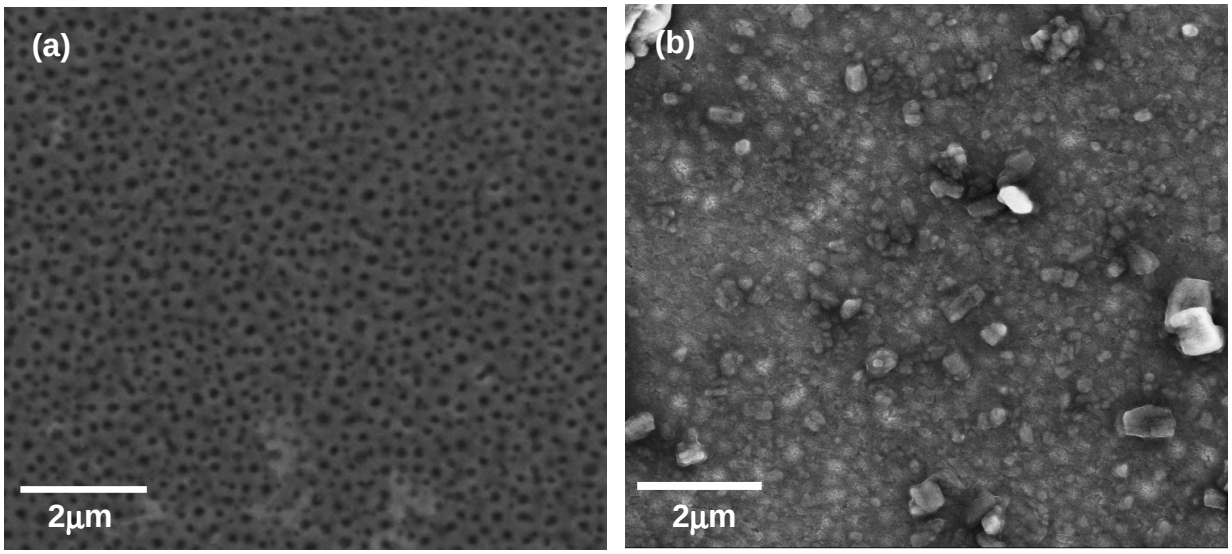

Figure 2

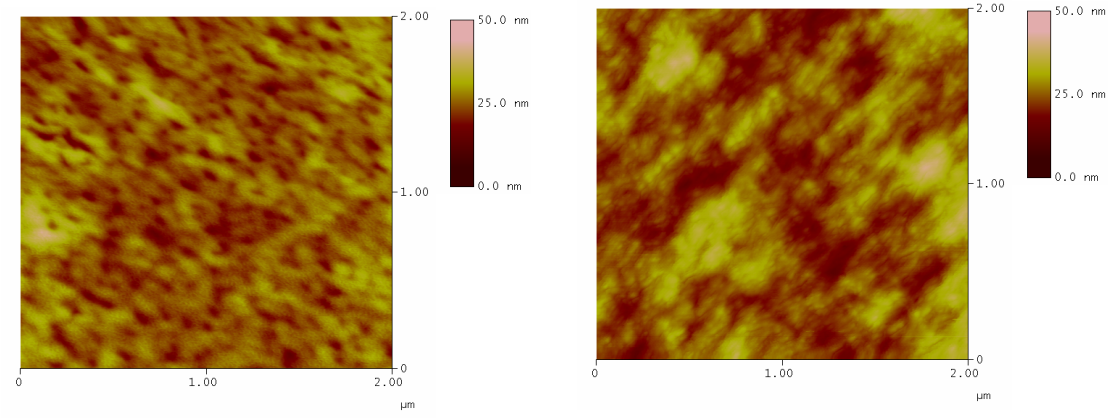

Figure 3

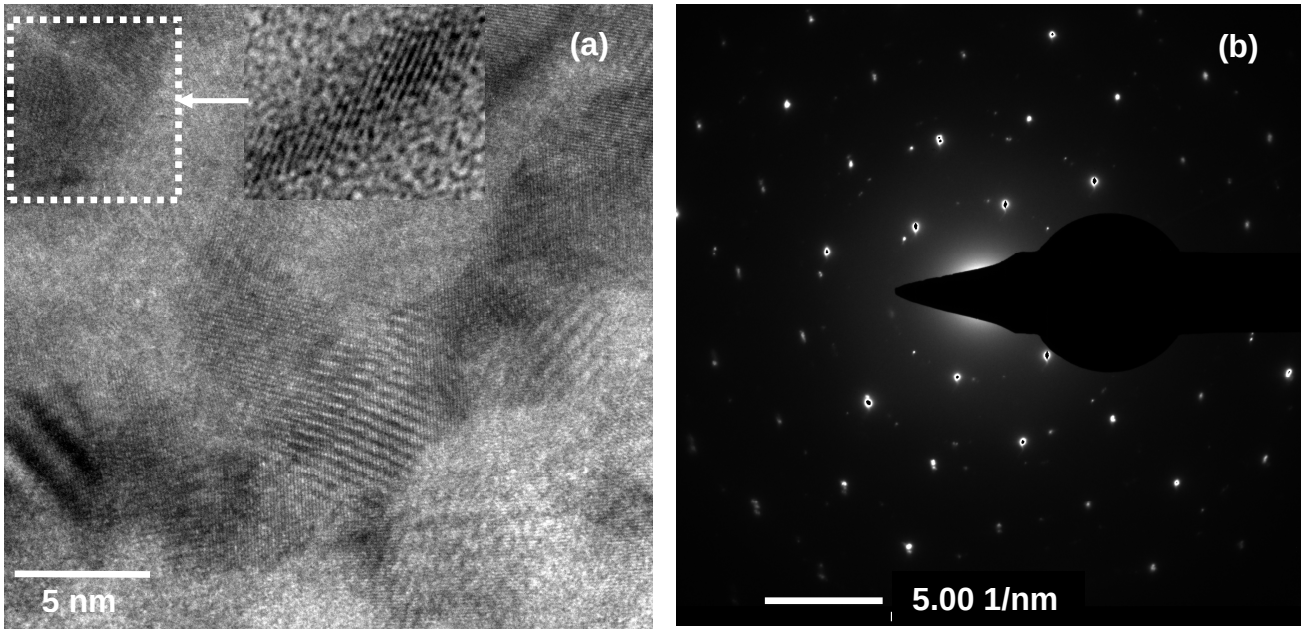

Figure 4

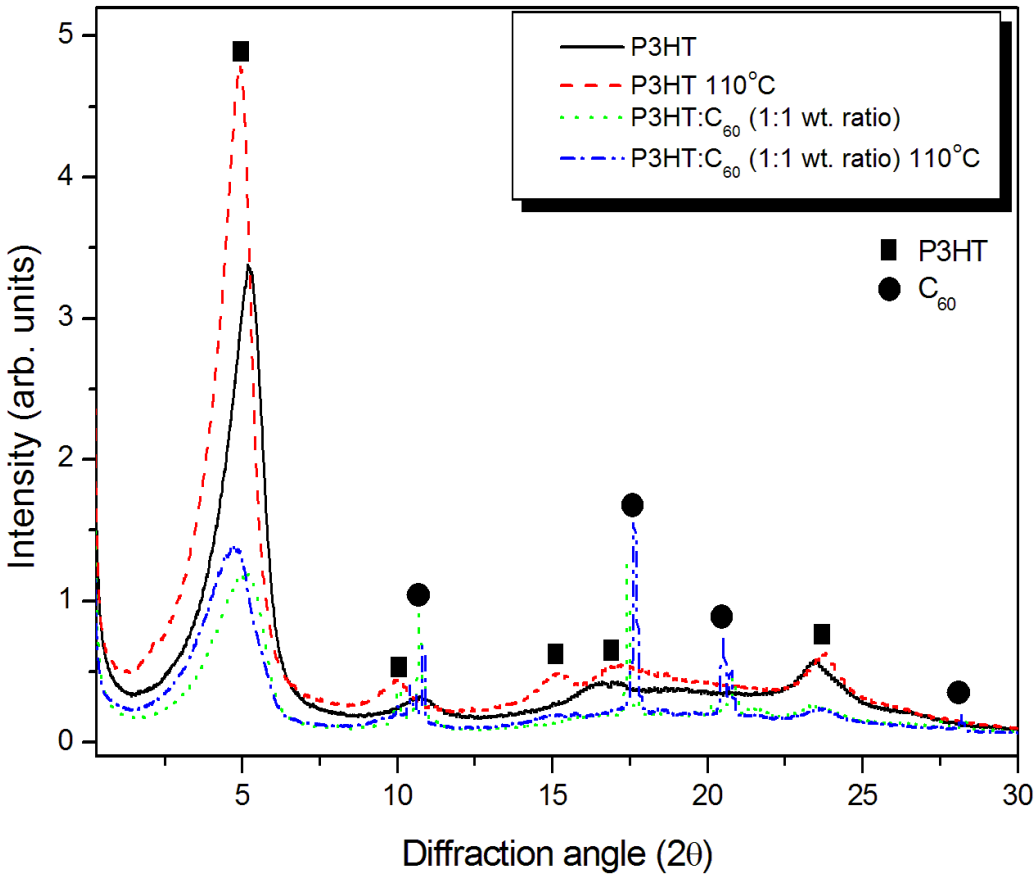
P3HT
P3HT 110°C
P3HT:C60 (1:1 wt. ratio)
P3HT:C60 (1:1 wt. ratio) 110°C
P3HT
C60
Intensity (arb. units)
Diffraction angle (2θ)
0
1
2
3
4
5
5
10
15
20
25
30

Figure 5

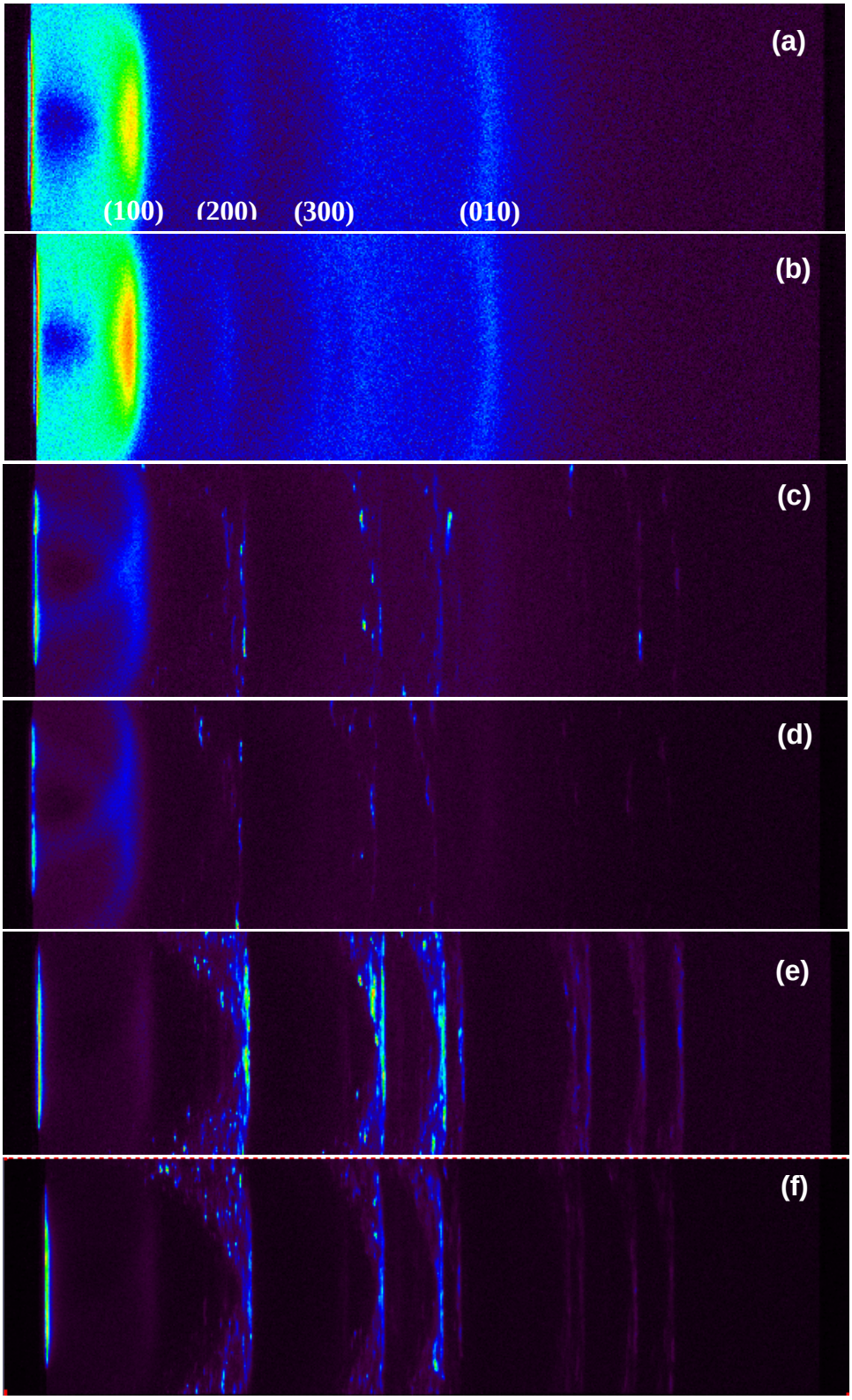

Figure 6

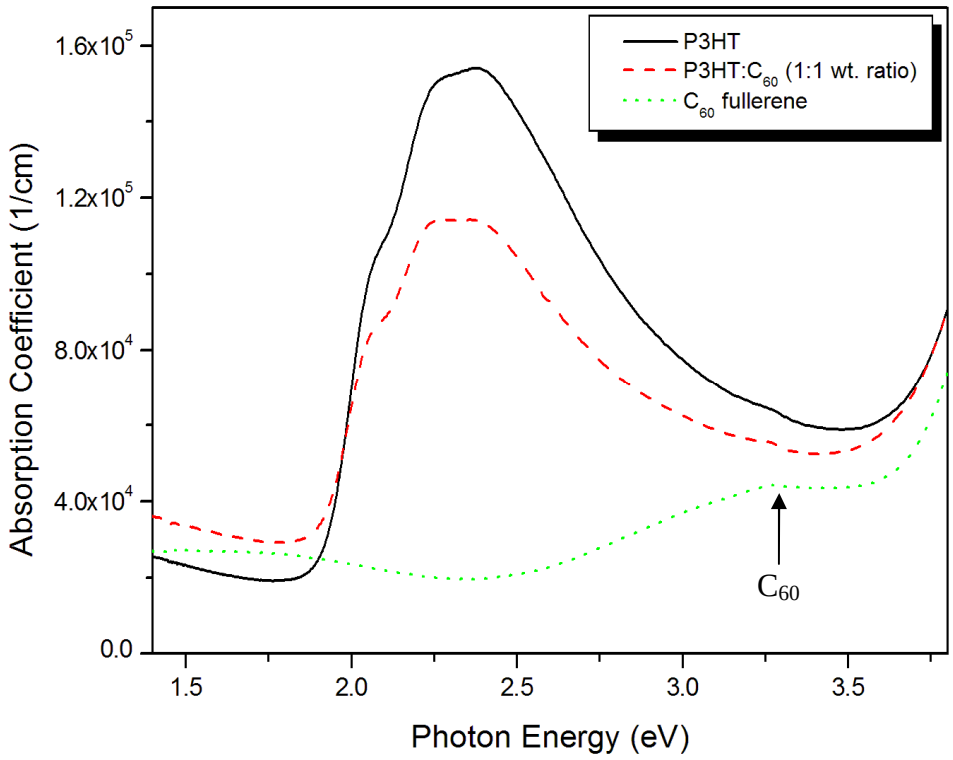
P3HT
P3HT:C60 (1:1 wt. ratio)
C60 fullerene
Absorption Coefficient (1/cm)
1.6x10^5
1.2x10^5
8.0x10^4
4.0x10^4
0.0
1.5
2.0
2.5
3.0
3.5
Photon Energy (eV)
C60

Figure 7

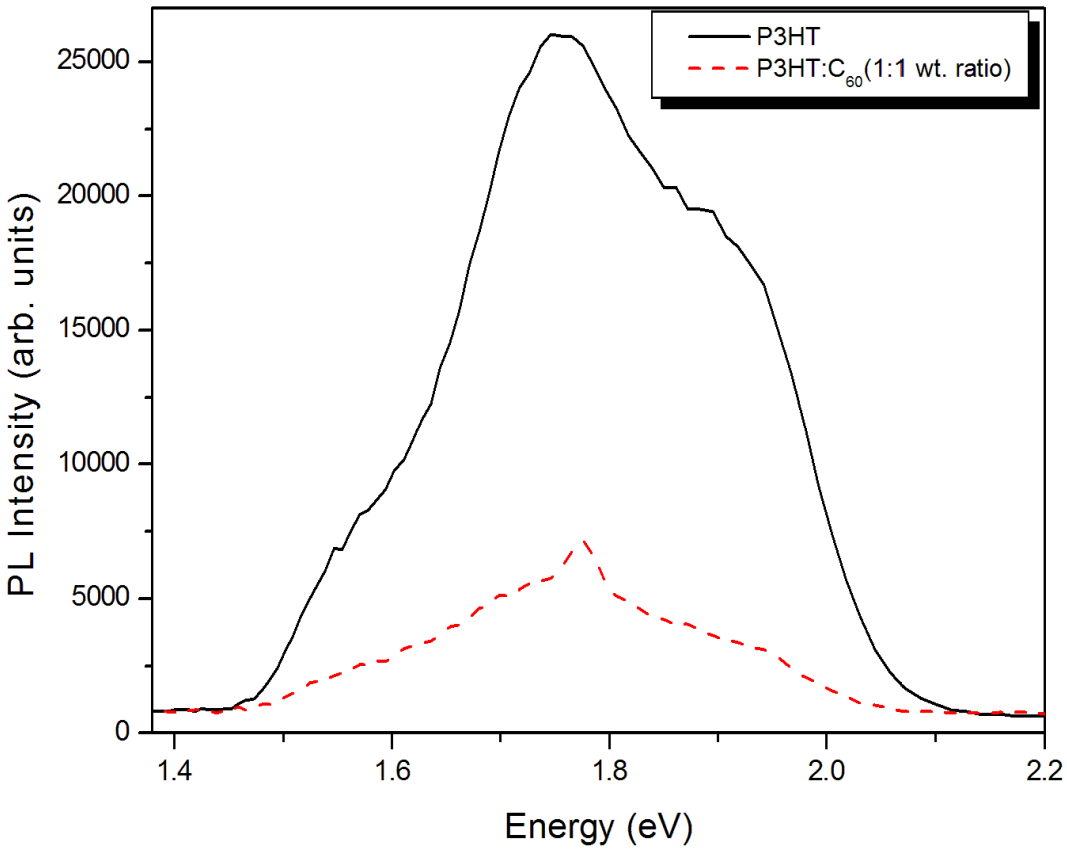

Figure 8

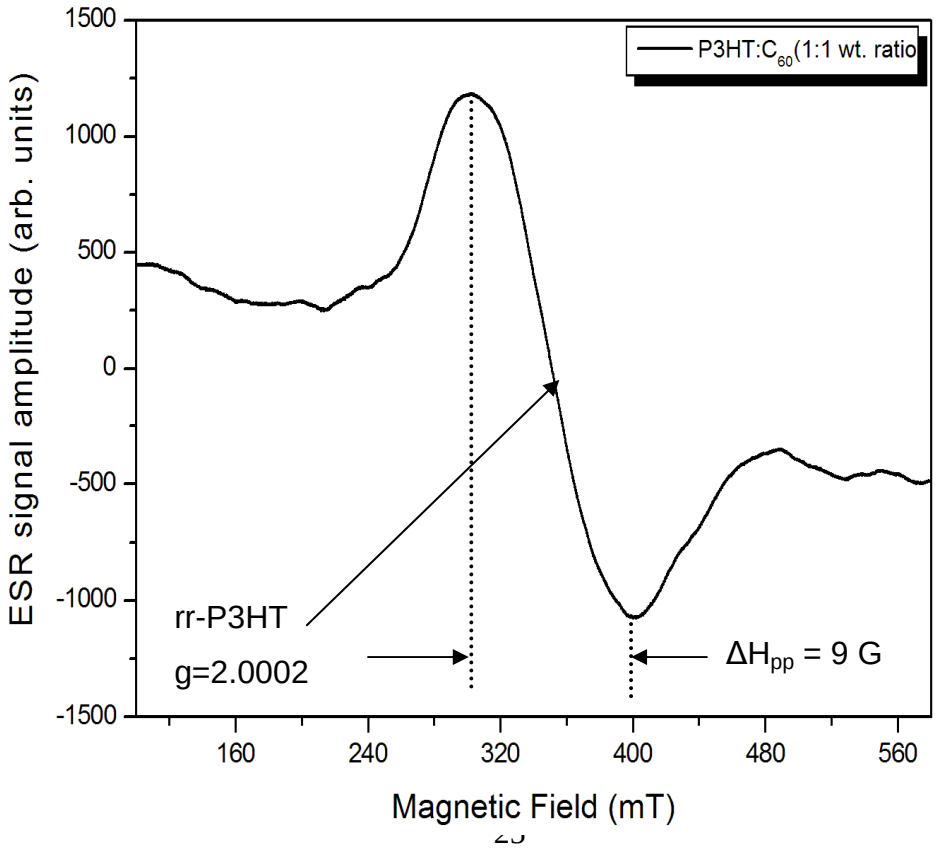

Figure 9

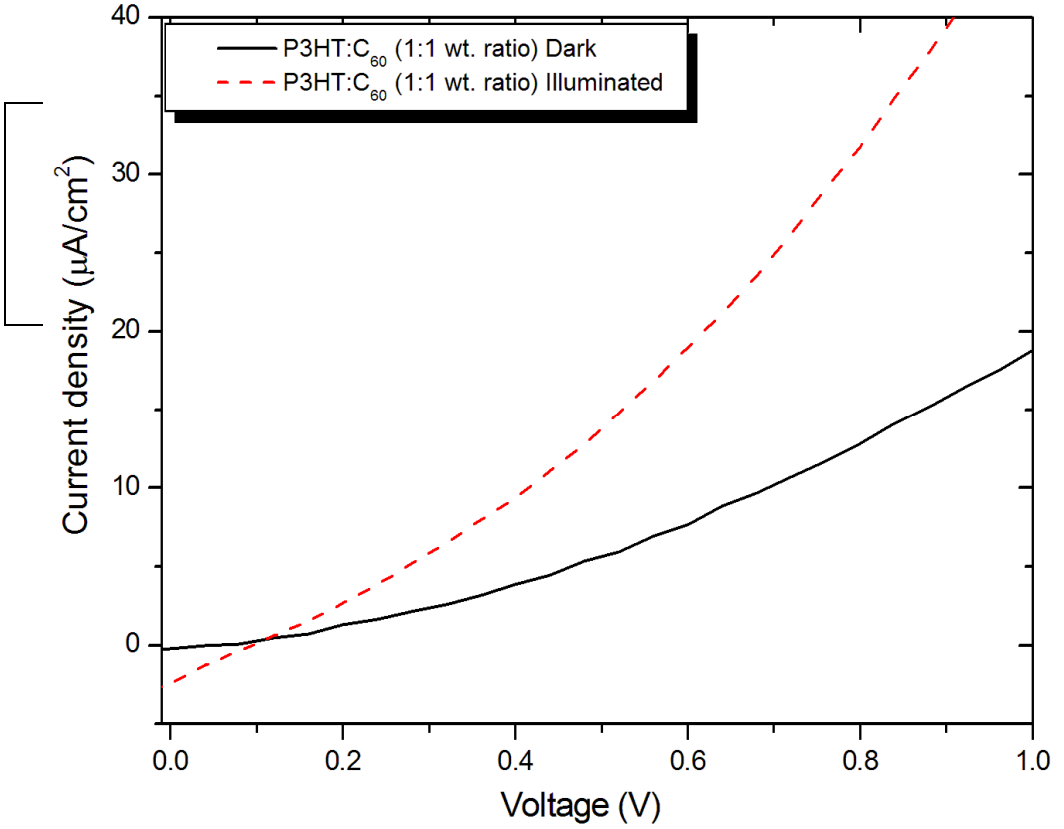

Table 1

	d-spacing (nm)	FWHM (nm)	Grain sizes (nm)	d-spacing (nm)	FWHM (nm)	Grain sizes (nm)
(100)	1.70	1.38	5.80	1.87	1.26	6.32
(200)	0.83	1.41	5.73	0.90	1.01	7.99
(300)	0.54	3.60	2.29	0.55	2.49	3.32
(010)	0.38	1.53	5.66	0.37	1.25	6.94